Coordination Chemistry Reviews, 97 (1990) 23–34
Elsevier Science Publishers B.V., Amsterdam — Printed in The Netherlands

ENERGETICS AND DYNAMICS OF SOLVENT REORGANIZATION IN CHARGE-TRANSFER EXCITED STATES

Mariusz Kozik, Norman Sutin, and Jay R. Winkler

Chemistry Department, Brookhaven National Laboratory, Upton, NY 11973

SUMMARY

The dynamics of solvation of the $Ru(bpy)_2(CN)_2$ metal-to-ligand charge-transfer excited state have been examined in a series of aliphatic alcohols. Steady-state emission spectra recorded at low temperature ($\approx$ 10 K) and at room temperature were used to resolve internal-mode and solvent contributions to the emission bandshape. Time-resolved emission spectra were fit to a model that takes into account internal-mode distortions as well as time-dependent broadening and shifts in emission maxima. A single-exponential solvent relaxation function does not adequately describe the temporal development of the emission profile of $Ru(bpy)_2(CN)_2$ in alcohols. The evolution of the emission spectrum is clearly biphasic, and can be reasonably fit with a biexponential function. The slower of the two relaxation times is comparable to the longest longitudinal relaxation time reported for the bulk solvent. These slower components, however, represent less than half of the overall approach to equilibrium. Local heating due to above-threshold excitation, and local solvent relaxation are two likely sources of the faster dynamics.

INTRODUCTION

Electronic absorption and emission spectroscopies have long been used to probe the environment of molecules in solution (ref. 1). The energies and shapes of absorption and emission profiles can be correlated with solvent properties and empirical solvent parameters to provide insight into the nature of solvation. With the advent of fast laser spectroscopic methods, the dynamics of solvation are also amenable to study. Time-resolved emission spectroscopy (TRES) is a particularly powerful technique that is being used to examine the dynamics of microscopic solvation of excited molecules, as well as the solvent dynamics associated with fast electron-transfer processes (refs. 2–8).

If just solvent nuclei change their equilibrium positions upon electronic excitation of a molecule in solution, then the energy of the steady-state absorption or emission maximum directly reflects the difference in position along the solvent coordinate of the initial and final states. Similar information is contained in the breadths of the bands. When internal-mode distortions accompany electronic excitation, it becomes

0010-8545/90/$04.20 © 1990 Elsevier Science Publishers B.V.

more difficult to extract information about the solvent configuration since the bandshape also reflects internal-mode rearrangements. In an attempt to factor-out internal-mode contributions, we have performed a Franck-Condon analysis of the room temperature and low temperature ($\approx$ 10 K) steady-state emission spectra of $Ru(bpy)_2(CN)_2$ in alcohol solvents.

Because electrons move much faster than nuclei, a short laser pulse can be used to prepare a molecule in a nonequilibrium solvation environment. Following excitation, the solvent will rearrange to accommodate the new permanent dipole of the excited molecule. Since the position and shape of the emission band reflect, in part, the solvation environment, the time evolution of the emission profile can be used to monitor the dynamics of microscopic solvation. We have examined the picosecond time-resolved emission spectra of $Ru(bpy)_2(CN)_2$ in alcohols at -20 °C and, using information from the analysis of the steady-state emission spectra, evaluated the dynamics of solvation of its metal-to-ligand charge-transfer (MLCT) excited state.

METHODS

Materials

HPLC-grade methanol (MeOH), n-propanol (n-PrOH), and n-butanol (n-BuOH), and absolute ethanol (EtOH) were refluxed over Na, distilled, and stored under Ar over molecular sieves (3A for MeOH, 4A for higher alcohols). *cis*-$Ru(bpy)_2(CN)_2$ was prepared and purified according to published procedures (refs. 9–10). Purity was judged by TLC on silica, developed with methanol.

Data Collection

Steady-state emission spectra. Emission spectra were recorded on an instrument constructed at Brookhaven National Laboratory (ref. 11). Samples for low-temperature spectra were held in sealed 4-mm OD fused-silica tubes and mounted on the cold head of a closed-cycle refrigerator. Identical configurations were used for both room-temperature and low-temperature spectra.

Time-resolved emission spectra. Picosecond time-resolved emission spectra were recorded following excitation with a 30-ps pulse from the third harmonic (355 nm) of a flashlamp-pumped, actively/passively mode-locked Nd:YAG laser. Emitted light was dispersed by a spectrograph and directed to the entrance slit of a streak camera. The instrument respsonse time was 35–40 ps (ref. 11).

Data Analysis

Steady-state emission spectra. The total spontaneous emission probability per unit time, w, is given by eq. 1 (ref. 12):

$$w = \int \left[\frac{n^3}{\epsilon} \left(\frac{E_e}{E} \right)^2 \right] \frac{64\pi^4 \nu^3}{c^3} I_{ab}(\nu) d\nu \qquad (1)$$

in which n is the refractive index and ϵ is the dielectric constant, both at frequency ν; E_e is the effective electric field at the chromophore and E is the macroscopic electric field; c is the speed of light; and $I_{ab}(\nu)$ is the emission probability per unit frequency interval at frequency ν for the electronic transition from state a to state b. The function $I_{ab}(\nu)$ is given by eq. 2:

$$I_{ab}(\nu) = Av_m \sum_n |\langle \Psi_{am} | M_{ab} | \Psi_{bn} \rangle|^2 \, \delta(E_{am} - E_{bn} - h\nu) \tag{2}$$

in which Av_m indicates a Boltzmann average over initial states Ψ_{am}; $\sum_n$ is a sum over all final states Ψ_{bn}; M_{ab} is the dipole transition operator; and δ is the Dirac delta function. Internal-mode distortions can be treated as harmonic oscillators both quantum mechanically and semiclassically, while solvent reorientation is generally described classically. Invoking the Condon approximation then leads to eq. 3:

$$I_{ab}(\nu) = \langle M_{ab} \rangle \prod_i \left\{ \sum_{m_i} exp\left(-\frac{m_i \hbar \omega_i}{k_B T} \right) \sum_{n_i} |\langle \chi_{am_i} | \chi_{bn_i} \rangle|^2 \, g(n, m, \nu) \right\} \tag{3}$$

in which the repeated product extends over the quantum-mechanical modes and χ_{jp_k} is the wavefunction for mode k in vibrational state p of the electronic state j. The squares of the vibrational overlap integrals, i.e., the Franck-Condon factors, are given by recursion relations for the Hermite polynomials (ref. 13), and it has been assumed that the vibrational frequency ω_i is the same in states a and b. The lineshape function is taken to be Gaussian and to contain broadening contributions from both the internal semiclassical modes and the classical solvent mode (eqs. 4–6, ref. 14).

$$g(n, m, \nu) = \left(\frac{\pi}{\sigma} \right) exp\left\{ \frac{-[E(n, m) - \lambda_S - h\nu]^2}{\sigma^2} \right\} \tag{4}$$

$$\sigma^2 = 4\lambda_S RT + 2 \sum_j (\lambda_{Ij} \hbar \omega_j) coth\left(\frac{\hbar \omega_j}{2 k_B T} \right) \tag{5}$$

$$E(n, m) = E_{00} - \sum_j \lambda_{Ij} + \sum_i (m_i - n_i) \hbar \omega_i \tag{6}$$

The term λ_S is the reorganization parameter for the classical solvent mode and the λ_{Ij} are the reorganization parameters for the classical internal modes. The sums over j include modes treated semiclassically, and the sum over i includes the quantum-mechanical modes. E_{00} is the electronic origin for the a-to-b transition.

Time-resolved emission spectra. Time-dependent spectral shifts arise because the solvent configuration is a function of time. In order to account for this time dependence, the spectral lineshape function can be recast according to eqs. 7–8 (refs. 3, 15).

$$g(n,m,\nu,t) = \left(\frac{\pi}{\sigma(t)}\right) exp\left\{\frac{-[E(n,m) - \lambda_S(1-2\rho(t)) - h\nu]^2}{\sigma(t)^2}\right\} \tag{7}$$

$$\sigma(t)^2 = 4\lambda_S RT\left[\frac{2\lambda_S RT(1-\rho(t)^2)+\sigma_0^2}{2\lambda_S RT+\sigma_0^2}\right] + 2\sum_j(\hbar\omega_j)coth\left(\frac{\hbar\omega_j}{2k_BT}\right) \tag{8}$$

The term σ_0^2 is the breadth of the energy distribution of excited molecules along the solvent coordinate at $t = 0$. The function $\rho(t)$ describes relaxation of the excited molecules along the solvent coordinate, and is the object of this study.

If quantum modes are ignored, it can be seen that the emission band is described by $g(n,m,\nu,t)$ and that the peak maximum will vary with time as $\rho(t)$. This shift is generally described by the correlation function $C(t)$ given by eq. 9 (refs. 4–7).

$$C(t) = \frac{\langle\nu(t)\rangle - \langle\nu(\infty)\rangle}{\langle\nu(0)\rangle - \langle\nu(\infty)\rangle} \tag{9}$$

In this approximation the experimental function $C(t)$ is equivalent to $\rho(t)$. Inclusion of quantum modes and broadening in $g(n,m,\nu,t)$ produces a far more complex time-evolution of the spectrum. If internal-mode distortion parameters are known, however, then time-resolved spectra can be fit to eqs. 3–8 using an assumed form for $\rho(t)$.

RESULTS

Steady-state emission spectra. The room-temperature and low-temperature emission spectra of $Ru(bpy)_2(CN)_2$ in ethanol are shown in Figure 1. At room temperature the emission profile is a broad, asymmetric band. At 12 K, a progression in a high energy vibrational mode resolves. The spectra were fit to the model described by eqs. 3–6 in which a single quantum mode was included and the remainder of the internal-mode broadening was treated semiclassically (dashed lines, Figure 1). This model, though only approximate, does provide an adequate description of the low-temperature and room-temperature spectra: the difference between the two is included as a distortion along the classical solvent coordinate.

The solvent reorganization parameter λ_S can be determined from the peak maximum of the emission profile or from its breadth (eqs. 4–5). By neglecting the temperature

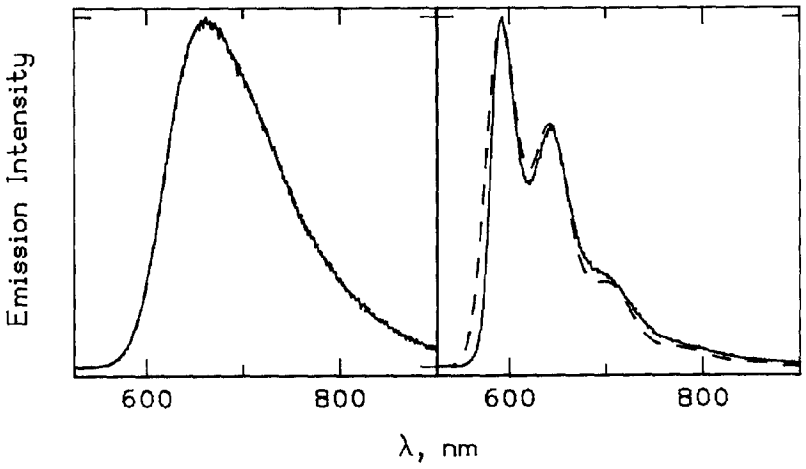

Figure 1. Emission spectra of $Ru(bpy)_2(CN)_2$ in EtOH. Left: room-temperature. Right: 12 K. Dashed lines are Franck-Condon fits to the spectra using one quantum mode.

dependence of the semiclassical modes, λ_S can be determined from the difference between σ^2 at the two temperatures. Alternatively, the difference in the maxima of $g(n, m, \nu)$ at the two temperatures should be equal to twice λ_S. Continuum models predict that the solvent reorganization parameter should be proportional to the dielectric function F_1 (eq. 10, ref. 16).

$$F_1 = \frac{3(\epsilon_0 - \epsilon_{op})}{[4(\epsilon_0 + 1)(\epsilon_{op} + 1)]} \tag{10}$$

ϵ_0 and ϵ_{op} are the static and optical dielectric constants of the solvent, respectively. The plots in Figure 2 of λ_S versus F_1 illustrate that the values determined from the breadths of the emission profiles correlate reasonably well with F_1, but those determined from peak-maxima data show an inverse correlation. The most likely explanation for this discrepancy is some temperature-dependence of the peak maximum that is not explicitly accounted for in eq. 4. The values of λ_S determined from the band widths are upper limits because of the neglect of the temperature dependence of the semiclassical modes.

Time-resolved spectra. The time-resolved emission spectra of $Ru(bpy)_2(CN)_2$ in n-BuOH at −20 °C are shown in Figure 3. The most striking aspect of these data is that the form of the emission decay function is wavelength-dependent. At shorter wavelengths, a large initial emission intensity rapidly decays to a smaller, constant value (on the 2-ns timescale). At longer wavelengths, a rapid increase in emission intensity

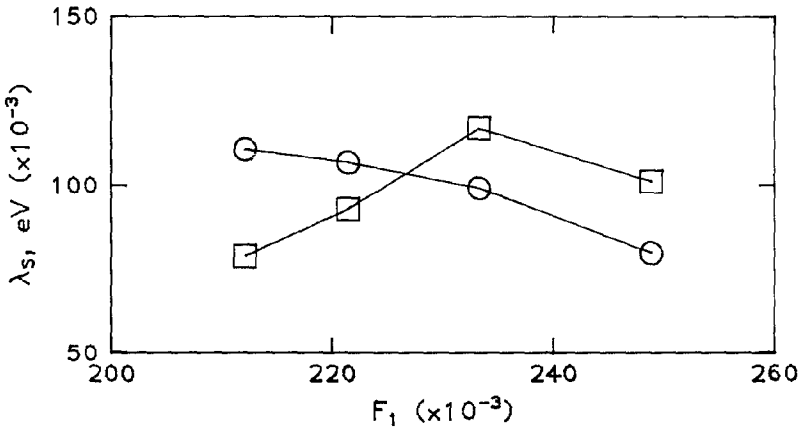

Figure 2. Plots of apparent λ_S versus the solvent dielectric function F_1. Values of λ_S were determined from emission maxima (O), and from breadths of emission bands (□).

follows excitation until a constant value is attained. Intermediate behavior is found at wavelengths between these two extremes. This behavior is consistent with an emission profile that shifts to the red following excitation. Similar behavior was found for $Ru(bpy)_2(CN)_2$ in MeOH, EtOH, and n-PrOH, though on different timescales.

As described above, the time-resolved emission spectra can be fit to the empirical correlation function, $C(t)$. Two-dimensional smoothing is effected by first fitting single-wavelength time-decays to multiexponential functions, then reconstructing time-resolved spectra which are fit to Gaussian distribution functions. The resulting $C(t)$ functions are decidedly nonexponential for $Ru(bpy)_2(CN)_2$ in EtOH, n-PrOH, and n-BuOH at -20 °C. A single exponential function describes $C(t)$ in MeOH at -20 °C, but it is likely that faster components are lost because of the limited time-resolution of the TRES apparatus. The parameters from the biexponential $C(t)$ fits are collected in Table 1.

The correlation function described by eq. 9 rigorously describes the relaxation along the solvent coordinate only if no internal-mode distortions accompany the a-to-b transition. It is possible, therefore, that the biphasic $C(t)$ decays arise from the complex spectral evolution set out in eqs. 3–8, rather than from a biphasic solvent relaxation function, $\rho(t)$. We examined this point by fitting the $Ru(bpy)_2(CN)_2$ time-resolved emission spectra to eqs. 3–8, using the internal-mode distortion parameters derived from the fits to the low-temperature emission spectra. The results of these fits are summarized in Table 1. Again, biexponential decay functions are necessary to describe the time-resolved spectra. The agreement between the peak-maximum fits and the Franck-Condon fits is

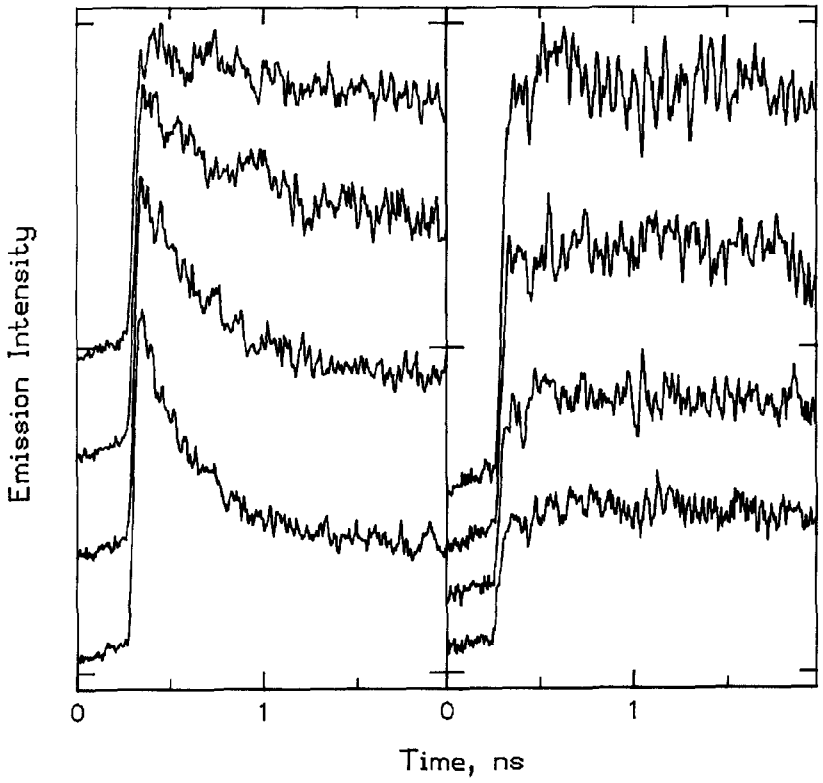

Figure 3. Wavelength dependence of time-resolved emission profiles of $Ru(bpy)_2(CN)_2$ in n-BuOH at −20 °C. Left, lower to upper: 607, 620, 634, 648 nm. Right, upper to lower: 661, 675, 689, 699 nm.

reasonably good. The major difference is that the time constant for the faster relaxation process is substantially smaller in the Franck-Condon fits. The source of this discrepancy could lie in the fact that in the Franck-Condon fits the position and shape of the $t = 0$ spectrum are fixed, while in the peak-maximum fits the value of $\langle\nu(0)\rangle$ is free to float. In any event, both fitting procedures clearly indicate biphasic solvent relaxation dynamics.

DISCUSSION

Continuum models are generally the first recourse for discussions of solvation properties. As was shown in Figure 1, a dielectric continuum model adequately describes the breadths of the $Ru(bpy)_2(CN)_2$ steady-state emission profiles, but not the emission max-

Table 1
Kinetic parameters for solvent relaxation in the MLCT excited state of $Ru(bpy)_2(CN)_2$.[a]

Solvent	C_1	τ_1	τ_2
MeOH	–	–	33
	0.88	5	30
EtOH	0.75	19	140
	0.77	5	70
n-PrOH	0.68	42	285
	0.70	2	202
n-BuOH	0.51	81	477
	0.50	6	429

[a] For biexponential relaxation functions, C_1 is the coefficient of the exponential with decay time τ_1, and $(1 - C_1)$ is the coefficient of the exponential with decay time τ_2. Decay times are in picoseconds. For each solvent, the upper set of parameters is from the peak-maximum analysis and the lower set is from the Franck-Condon analysis.

Table 2
Dielectric relaxation properties of aliphatic alcohols at 253 K.[a]

Alcohol	τ_{D3}	τ_{D2}	τ_{D1}	ϵ_{01}	$\epsilon_{\infty 1}$	τ_{L1}
MeOH	–	–	154	43.2	6.40	23
EtOH	–	–	632	31.4	4.85	98
n-PrOH	4	34	1920	27.4	3.92	274
n-BuOH	3.5	50	3145	23.6	3.65	486

[a] Relaxation times are in picoseconds (refs. 4e, 6f, 23).

ima. Specific solvation effects, especially hydrogen-bonding, can complicate the analysis, but the general trends can be described by bulk solvent properties. The dynamics of microscopic solvation have also been described by continuum models. In a Debye-type dielectric, the approach to equilibrium of the dielectric polarization following an instaneous change in the permanent dipole moment of a spherical solute is exponential, with a time-constant τ_L given by eq. 11 (refs. 17–20):

$$\tau_L = \left(\frac{\epsilon_\infty}{\epsilon_0}\right) \tau_D \tag{11}$$

where τ_D, the Debye-time, is the exponential time-constant for the approach to equilibrium polarization following an instantaneous change in the external electric field (refs.

21, 22). The high and low frequency dielectric constants, ϵ_∞ and ϵ_0, arise from the dielectric dispersion of the medium.

Alcohols are not simple Debye solvents, and are reported to have three regions of dielectric dispersion. The highest frequency component is attributed to rotation of free hydroxyl groups, the mid-range component to reorientation of free alcohol molecules, and the low-frequency component to disruption of hydrogen-bonds in alcohol aggregates (Table 2, ref. 23). In MeOH, EtOH, n-PrOH, and n-BuOH, the low-frequency process accounts for the major part of the dielectric constant. The definition of τ_L for alcohols is also complicated. A different value of ϵ_∞ is associated with each of the three regions of dielectric dispersion. These values differ from the optical dielectric constant ϵ_{op}, which is equal to the square of the refractive index of the medium, and which is commonly used for ϵ_∞ in nonassociated solvents. The significance of this complication is especially clear in n-BuOH where, depending upon the choice of ϵ_∞, τ_L can vary by almost a factor of two ($\epsilon_{\infty 1} = 3.65$; $\epsilon_{op} = 1.96$). The τ_{L1} values in Table 2 were calculated from eq. 11 by using the ϵ_{01}, $\epsilon_{\infty 1}$, and τ_{D1} values in reference 6f ($\epsilon_{\infty 1}$ refers to the lowest frequency region of dielectric dispersion, i.e., $\tau_{D1} > \tau_{D2} > \tau_{D3}$). In light of the complex dielectric relaxation behavior of the alcohols it is not surprising that the solvent relaxation dynamics for the $Ru(bpy)_2(CN)_2$ MLCT excited state are biphasic. Comparison of the data in Tables 1 and 2 reveals that the slower solvent relaxation time (τ_2) is in fair accord with the low-frequency longitudinal dielectric relaxation time (τ_{L1}) for the four alcohols that have been examined. The contributions of the two relaxation times to their corresponding relaxation functions, however, are quite different. While the dispersion region with time constant τ_{L1} corresponds to the largest part of the dielectric constant in these alcohols, τ_2 represents less than half of the observed microscopic solvation dynamics.

The most obvious explanation of the above data is a breakdown of the dielectric continuum model. Most of the solvent reorganization associated with formation of the MLCT excited state is likely to be found in the first few solvation shells around the solute (refs. 4g, 6e, 24). In this region near the solute, however, the solvent reorientation dynamics are least likely to resemble bulk solvent dynamics. The problem could be particularly acute in alcohols where the solute will disrupt the hydrogen-bonded aggregates found in the bulk. A simple explanation of the observed solvent relaxation dynamics is that the faster decay times reflect relaxation of solvent nearer the solute, while the slower times arise from relaxation of more distant, bulk-like solvent.

Similar explanations have been proposed to explain the biphasic relaxation dynamics found for several organic chromophores in aprotic solvents (refs. 4–7). Unlike the results with alcohols, however, observed relaxation times fall in the range $\tau_D > \tau_{obsd} > \tau_L$. The Debye time is reported to be a better measure of individual molecule reorientation times than τ_L, and is expected to be a better approximation to the relaxation dynamics of solvent molecules nearer the solute (refs. 4g, 22). The obvious conclusion, then, is that

in these aprotic solvents, molecules farther from the solute relax *faster* than the solvent molecules nearby. The aggregation in alcohols is possibly responsible for their different behavior. Since solvent molecules in the immediate vicinity of the solute are not likely to be extensively aggregated, relaxation might resemble the individual alcohol-molecule reorientation times, τ_{D2}. Comparison to the τ_1 values in Table 1 reveals fair agreement with the corresponding values of τ_{D2}.

This simple explanation of the data in Table 1 must be tempered with a number of caveats. In the first instance, the $Ru(bpy)_2(CN)_2$ complexes were excited with laser pulses significantly above ($\approx$ 1.4 eV) the origin of the emission band. This excess energy is ultimately deposited into the solvent, leading to local heating which could complicate the solvent relaxation dynamics. The spectral models described above also include a number of assumptions. The most tenuous might be the Condon approximation which states that the transition dipole, and hence the electronic wavefunctions, are independent of all nuclear coordinates, including solvent. This may be a poor assumption because the wavefunction describing the MLCT excited state could depend directly upon the solvent orientation since the electric field experienced by the molecule will vary substantially with solvent orientation. It is well-known from Stark-effect spectroscopy that excited-state wavefunctions can be significantly perturbed by external electric fields (ref. 25). Fleming and coworkers have proposed a similar explanation for the rapid fluorescence depolarization dynamics found with coumarin 153 in alochol solvents (ref. 4c). A further serious complication involves the cyanide ligands of $Ru(bpy)_2(CN)_2$. Protic solvents are known to hydrogen-bond with cyano groups (ref. 26), and the magnitude of this interaction need not be identical in the ground and MLCT excited states. Hygrogen-bonding dynamics, therefore, might also be contributing to the observed solvent relaxation, but would not be described by bulk solvent dielectric properties.

CONCLUSIONS

Excitation of $Ru(bpy)_2(CN)_2$ in alcohol solvents to a thermally equilibrated MLCT excited state requires, depending upon the alcohol, 0.08–0.12 eV of solvent reorganization. At −20 °C this solvent reorientation proceeds on a subnanosecond timescale and the function describing solvent relaxation is biphasic. The models often used to describe these dynamics assume that the dielectric solvent is a uniform continuum up to the edge of a spherical solute. Since most of the solvent reorientation is likely to occur in the first few solvent shells, however, a reliable model must accurately describe solvent in the vicinity of the solute. Continuum models, therefore, are likely to be deficient in describing all aspects of solvent reorientation dynamics. The slower component of the $Ru(bpy)_2(CN)_2$ MLCT solvent relaxation is comparable to τ_{L1}, in agreement with the predictions of continuum theories. The faster, major component of the relaxation, however, probably arises from relaxation of solvent molecules nearer the solute, rep-

resenting a breakdown of the dielectric continuum model. We are continuing TRES studies of metal complexes in order to characterize further the parameters that control the dynamics of solvent reorientation about electronically excited solutes.

Acknowledgment. We thank Dr. Bruce Brunschwig for many helpful discussions, and for his assistance in the preparation of this manuscript. This research was carried out at Brookhaven National Laboratory under Contract DE–AC02–76CH00016 with the U. S. Department of Energy and supported by its Division of Chemical Sciences, Office of Basic Energy Sciences.

REFERENCES

1. (a) N.S. Bayliss, E.G. McRae, J. Phys. Chem. 58 (1954), 1813–1822; (b) Y. Ooshika, J. Phys Soc., Japan 9 (1954), 594–602; (c) E. Lippert, Z. Naturforsch. 10a (1955), 541–545; (d) N. Mataga, Y. Kaifu, M. Koizumi, Bull. Chem. Soc., Japan 29 (1956), 465–470; (e) E.G. McRae, J. Phys. Chem. 61 (1957), 562–572; (f) E. Lippert, Z. Electrochem. 61 (1957), 962–975; (g) N. Mataga, Bull. Chem. Soc., Japan 36 (1963), 654–662; (h) N. G. Bakhshiev, Opt. Spect. 16 (1964), 446–451; (i) N. G. Bakhshiev, I. V. Piterskaya, Opt. Spect. 19 (1965), 390–395; (j) R. W. Taft, N. J. Pienta, M. J. Kamlet, E. M. Arnett, J. Org. Chem. 46 (1981), 661–667; (k) J. E. Brady, P. W. Carr, J. Phys. Chem. 89 (1985), 5759–5766.
2. (a) W.R. Ware, S.K. Lee, G.J. Brant, P.P. Chow, J. Chem. Phys. 54 (1971), 4729–4737; (b) S.K. Chakrabat, W.R. Ware, J. Chem. Phys. 55 (1971), 5494–5498; (c) W.R. Ware, P.P. Chow, S.K. Lee, Chem. Phys. Lett. 2 (1986), 356–358.
3. (a) Y.T. Mazurenko, Opt. Spect. 36 (1974), 283–286; (b) Y.T. Mazurenko, Opt. Spect. 44 (1978), 417–420; (c) Y.T. Mazurenko, Opt. Spect. 45 (1978), 141–145; (d) Y.T. Mazurenko, Opt. Spect. 45 (1978), 765–767; (e) Y.T. Mazurenko, Opt. Spect. 48 (1980), 388–392.
4. (a) B. Bagchi, D.W. Oxtoby, G.R. Fleming, Chem. Phys. (1984), 257–267; (b) E.W. Castner, M. Maroncelli, G.R. Fleming, J. Chem. Phys. 86 (1987), 1090–1097; (c) M. Maroncelli, G.R. Fleming, J. Chem. Phys. 86 (1987), 6221–6239; (c) E.W. Castner, G.R. Fleming, B. Bagchi, Chem. Phys. Lett. 143 (1988), 270–276; (d) M. Maroncelli, G.R. Fleming, J. Chem. Phys. 89 (1988), 875–881; (e) E.W. Castner, Jr., B. Bagchi, M. Maroncelli, S.P. Webb, A.J. Ruggiero, G.R. Fleming, Ber. Bunsenges. Phys. Chem. 92 (1988), 363–372; (f) E.W. Castner, G.R. Fleming, B. Bagchi, M. Maroncelli, J. Chem. Phys. 89 (1988), 3519–3534; (g) M. Maroncelli, J. MacInnis, G.R. Fleming, Science 243 (1989), 1674–1681.
5. N. Kitamura,H.-B. Kim, Y. Kawanishi, R. Obata, S. Tazuke, J. Phys. Chem. 90 (1986), 1488–1491.
6. (a) S.-G. Su, J.D. Simon, J. Phys. Chem. 90 (1986), 6475–6479; (b) S.-G. Su, J.D. Simon, J. Phys. Chem. 91 (1987), 2693–2696; (c) J.D. Simon, S.-G. Su, J. Chem. Phys. 87 (1987), 7016–7023; (d) J.D. Simon, S.-G. Su, J. Phys. Chem. 92 (1988), 2395–2397; (e) O. Karim, A.D.J. Haymet, M.J. Banet, J.D. Simon, J. Phys. Chem. 92 (1988), 3391–3394; (f) S.-G. Su, J.D. Simon, J. Chem. Phys. 89 (1988), 908–919; (g) J.D. Simon, Acc. Chem. Res. 21 (1988), 128–134; (h) S.G. Su, J.D. Simon, Chem. Phys. Lett. 158 (1989), 423–428.
7. (a) M.A. Kahlow, T.J. Kang, P.F. Barbara, J. Phys. Chem. 91 (1987), 6452–6455; (b) V. Nagarajan, A.M. Brearly, T.J. Kang, P.F. Barbara, J. Phys. Chem. 86 (1987),

3183–3196; (c) M.A. Kahlow, T.J. Kang, P.F. Barbara, J. Chem. Phys. 88 (1988), 2372–2378; (d) T.J. Kang, M.A. Kahlow, D. Giser, S. Swallen, V. Nagarajan, J. Wlodzimierz, P.F. Barbara, J. Phys. Chem. 92 (1988), 6800–6807; (e) J. Wlodzimierz, G.C. Walker, A.E. Johnson, M.A. Kahlow, P.F. Barbara, J. Phys. Chem. 92 (1988), 7039–7041; (f) M.A. Kahlow, J. Wlodzimierz, T.J. Kang, P.F. Barbara, J. Chem. Phys. 90 (1989), 151–158.

8. (a) S. Kinoshita, N. Nishi, T. Kushida, Chem. Phys. Lett. 134 (1987), 605–609; (b) S. Kinoshita, N. Nishi, J. Chem. Phys. 89 (1988), 6612–6622.
9. J.N. Demas, T.F. Turner, G.A. Crosby, Inorg. Chem. 8 (1969), 674–675.
10. A.S. Schilt, Inorg. Chem. 3 (1964), 1323–1325.
11. M. Kozik, N. Sutin, J. Winkler, in preparation.
12. M. Lax, J. Chem. Phys. 20 (1952), 1752–1760.
13. F. Ansbacher, Z. Naturforsch. 14a (1959), 889–892.
14. C.J. Ballhausen, "Molecular Electronic Structures of Transition Metal Complexes," McGraw-Hill Inc., New York, (1979), pp. 125–128.
15. (a) R.F. Loring, Y.J. Yan, S. Mukamel, Chem. Phys. Lett. 135 (1987), 23–29; (b) Y.J. Yan, S. Mukamel, J. Chem. Phys. 86 (1987), 6085–6107; (c) R.F. Loring, S. Mukamel, J. Chem. Phys. 87 (1987), 1272–1283; (d) R.F. Loring, Y.J. Yan, S. Mukamel, J. Chem. Phys. 87 (1987), 5840–5857; (e) M. Sparpaglione, S. Mukamel J. Phys. Chem. 91 (1987), 3938–3943; (f) M. Sparpaglione, S. Mukamel, J. Chem. Phys. 88 (1988), 1465–1466; (g) M. Sparpaglione, S. Mukamel, J. Chem. Phys. 88 (1988), 3263–3280; (h) M. Sparpaglione, S. Mukamel, J. Chem. Phys. 88 (1988), 4300–4311.
16. B.S. Brunschwig, S. Ehrenson, N. Sutin, J. Phys. Chem. 91 (1987), 4714–4723.
17. (a) G. van der Zwan, J.T. Hynes, Physica 121A (1983), 227–252; (b) G. van der Zwan, J.T. Hynes, Chem. Phys. Lett. 101 (1983), 367–371; (c) G. van der Zwan, J.T. Hynes, J. Phys. Chem. 89 (1985), 4181–4188; (d) J.T. Hynes, J. Phys. Chem. 90 (1986), 3701–3706.
18. (a) D.F. Calef, P.G. Wolynes, J. Phys. Chem. 87 (1983), 3387–3400; (b) D.F. Calef, P.G. Wolynes, J. Chem. Phys. 78 (1983), 470–482.
19. (a) H. Sumi, R.A. Marcus, J. Chem. Phys.1986 84, 4272–4276; (b) H. Sumi, R.A. Marcus, J. Chem. Phys. 84 (1986), 4894–4914; (c) W. Nadler, R.A. Marcus, J. Chem. Phys. 86 (1987), 3906–3924.
20. (a) B. Bagchi, A. Chandra, Chem. Phys. Lett. 155 (1989), 533–538; (b) B. Bagchi,A. Chanfra, J. Chem. Phys. 90 (1989), 7338–7345.
21. H. Frölich, "Theory of Dielectrics. Dielectric Constant and Dielectric Loss," Oxford University Press, London, (1958), pp. 71–72.
22. H.L. Friedman, J. Chem. Soc., Faraday Trans 2 79 (1983), 1465.
23. S.K. Garg, C.P. Smyth, J. Phys. Chem. 69 (1965), 1294–1301.
24. (a) R.A. Kuharski, J.S. Bader, D. Chandler, M. Sprik, M.L. Klein, R.W. Impey, J. Chem. Phys. 89 (1988), 3248–3257; (b) J.S. Bader, D. Chandler, Chem. Phys. Lett. 157 (1989), 501–504.
25. D.H. Oh, S. Boxer, J. Am. Chem. Soc. 111 (1989), 1130–1131.
26. (a) H.E. Toma, M.A. Takasugi, J. Solution Chem. 12 (1983), 547–561; (b) P. Belser, A. von Zelewsky, A. Juris, F. Barigelletti, V. Balzani, Gazz. Chim. Ital. 115 (1985), 723–729.